JOURNAL OF CATALYSIS

ELSEVIER

New aspects for heterogeneous cobalt-catalyzed hydroamination of ethanol

A.K. Rausch [a], E. van Steen [b], F. Roessner [a],*

[a] *Industrial Chemistry 2, University of Oldenburg, 26111 Oldenburg, Germany*
[b] *Catalysis Research Centre, Department of Chemical Engineering, University of Cape Town, Private Bag X3, Rondebosch 7701, South Africa*

Abstract

Gas-phase hydroamination of ethanol and ammonia over supported cobalt on silica catalysts was investigated at 103 kPa. Besides the desired products, mono-, di- and triethylamine, acetonitrile, diethylimine, and hydrocarbons (methane, ethene, ethane, propane, and propene) were identified as byproducts. The formation of hydrocarbons was found to depend on the cobalt loading of the catalyst and on the pretreatment of the catalyst. Guaranteeing a sufficient reduction of the cobalt catalyst allows a reduction in the selectivity of hydrocarbons from 25 to 10 mol% at a constant conversion of 90%. In addition, rapid deactivation of the catalyst was observed in the absence of hydrogen. The deactivation was ascribed to the interaction of ammonia with the catalyst and is largely reversible. Carbonaceous species are present on the spent catalyst, as shown by temperature-programmed reduction. These species are thought to be responsible for a slow deactivation in the presence of hydrogen.
© 2007 Elsevier Inc. All rights reserved.

1. Introduction

Short-chain aliphatic amines (C_2–C_6) are important intermediates for the chemical and pharmaceutical industries. Numerous drugs, dyes, herbicides, and other compounds contain amino groups that are introduced by reaction with an amine [1]. The production of aliphatic amines is often performed by hydroamination, the conversion of an alcohol with ammonia or a primary or secondary amine in the presence of hydrogen. A typical heterogeneous catalyst for hydroamination contains metallic cobalt, nickel or copper supported on silica or alumina. The conversion of alcohol is believed to be metal-catalyzed, with activity for the conversion of the alcohol proportional to the metal surface area [2].

Due to the manifold applications of amines, hydroamination has been investigated using a variety of alcohols and amines or ammonia [3]. The hydroamination of ethanol with ammonia, the topic of the present study, was investigated by Sewell et al. [4] on cobalt catalysts and by Jones et al. [5] and Jackson et al. [6] on nickel catalysts. The results reported to date have

not demonstrated a single consistent mechanism, because they were achieved for a range of catalysts and educts under different reaction conditions. Two mechanisms are primarily discussed for the hydroamination of ethanol [3,5–7], both of which assume that the abstraction of the α-H-atom of the alcohol is the rate-determining step in amination. These mechanisms differ with respect to the nitrogen-containing intermediates adsorbed on the catalysts surface. Baiker et al. [7] investigated the kinetics of the amination of long-chain aliphatic alcohols with methylamines and proposed a reaction pathway with nitrogen-containing intermediates with a hydroxyl group (see Scheme 1). The intermediate amino alcohol is converted through elimination of the hydroxyl group and subsequent addition of hydrogen to amines. Jones et al. [5] and Jackson et al. [6] proposed a mechanism for the amination of ethanol with ammonia based on their experiments with nickel catalysts suggesting the formation of surface ethylidene [5] or ethyl [6] intermediates. The C–N bond is formed in a reaction between the chemisorbed amine or ammonia and an oxygen-free surface derivative of the alcohol (see Scheme 2). This mechanism yielded a better description for hydroamination of isotopic-labeled ethanol with ammonia. However, DFT calculations performed by Cheng et al. [8] showed that the mechanism proposed by Baiker et al. [7]

* Corresponding author. Fax: +49 0441 798 3360.
 E-mail address: frank.roessner@uni-oldenburg.de (F. Roessner).
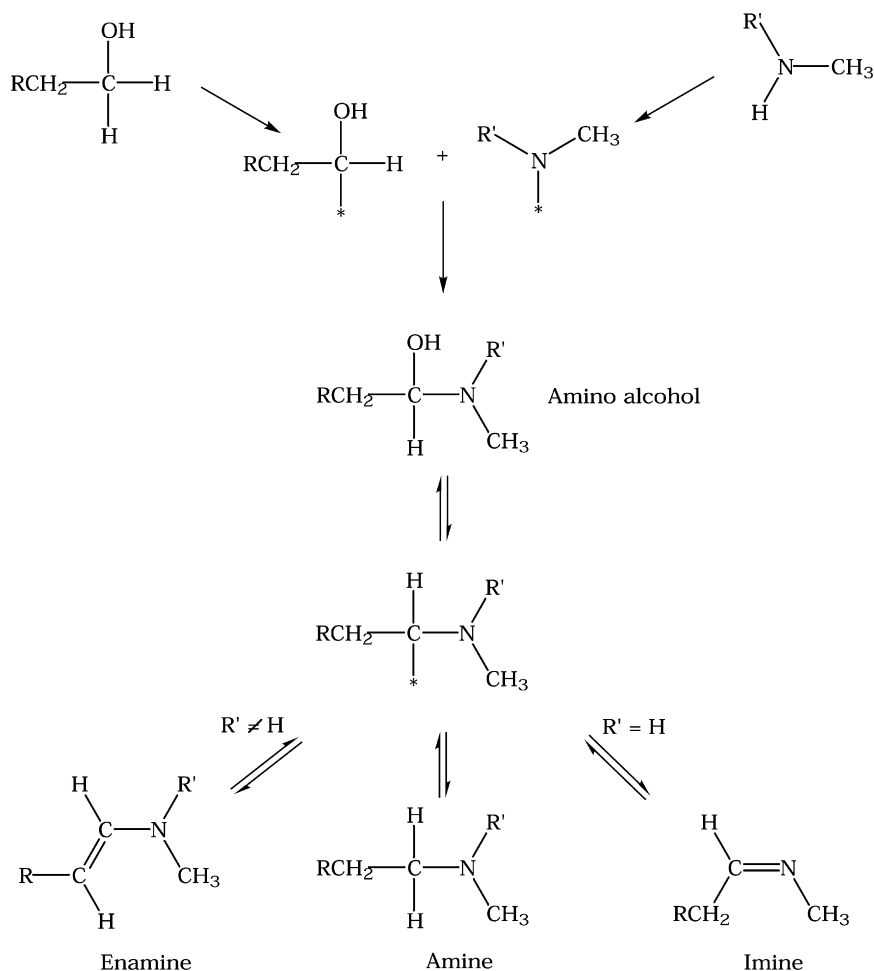
Scheme 1. Reaction pathway for amination of an aliphatic alcohol by a primary or secondary amine via hydroxygroup containing intermediates (∗, active site). Adapted from [5].
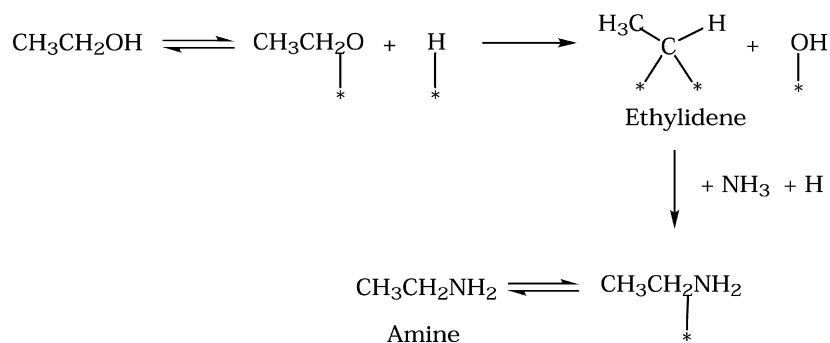
Scheme 2. Reaction pathway for amination of ethanol by ammonia via ethylidene intermediate. Adapted from [3].

is energetically slightly favored on nickel and cobalt catalysts, but both mechanisms may be operative at the same time under typical hydroamination conditions.

During hydroamination, various byproducts can be observed, including hydrocarbons [9–11], nitriles [10], imines [10] and enamines [7]. The formation of hydrocarbons, which is ascribed to the hydrogenolysis of amines [10,11], is particularly undesirable. The formation of other products might be the result of successive dehydrogenation of the product amines. Selectivity of amines and byproducts strongly depends on such reaction parameters as feed composition, temperature, and hydrogen partial pressure. The affect of feed composition, temperature (between 140 and 200 °C), and hydrogen partial pressure on the amination of ethanol has been investigated [4]; however, a detailed analysis of the byproducts has not been conducted.

Copper, nickel, and cobalt catalysts may deactivate in alcohol hydroamination. Mechanisms have been proposed for the deactivation of these catalysts via formation of metal nitrides, metal carbides, and carbonaceous deposits during the disproportionation of methylamines [11]. In addition, the influence

of hydrogen on catalyst deactivation and conversion of long-chain alcohols in liquid phase has been investigated for copper catalysts. However, the influence of hydrogen on the product selectivity has not been discussed [12].

In the present study, the hydroamination of ethanol was investigated on silica-supported cobalt catalysts as a model catalyst known to have catalytic activity in this reaction [4]. The investigation focused on the formation of hydrocarbons as byproducts and on deactivation of the catalysts.

2. Experimental

2.1. Catalyst preparation

Co/SiO$_2$ catalysts with different cobalt loadings were prepared by incipient wetness impregnation of silica gel (Sigma–Aldrich, $S_{BET} = 110$ m^2/g, $V_{pore} = 0.3$ cm^3/g) using an aqueous solution of Co(NO$_3$)$_2$·6H$_2$O (Fluka). The cobalt concentration was adjusted to yield metal loadings of 1, 5, 10, 15, and 20 wt%. After impregnation, the catalysts were dried at 100 °C for 16 h.

2.2. Catalyst characterization

The metal loading of the prepared catalysts was confirmed by atomic-absorption spectroscopy (AAS) using a Varian SpectraAA 300 spectroscope. The reducibility of the catalysts was investigated by temperature-programmed reduction (TPR) in hydrogen using a TPR apparatus (Raczek GmbH) with a thermal conductivity detector (TCD). The samples were oxidized in air at 500 °C before the TPR. The TPR was performed at 50 to 800 °C with a temperature ramp of 10 °C/min using 50 ml (NTP)/min of 5 vol% H$_2$ in argon as the reduction gas.

2.3. Hydroamination of ethanol

The amination of ethanol was performed in fixed-bed reactor at atmospheric pressure. For the catalytic experiment, a nitrogen flow (14 ml (NTP)/min) was saturated with ethanol at 36 °C, resulting in a flow rate of gaseous ethanol of 2.3 ml (NTP)/min. The ammonia flow rate was always 7 ml (NTP)/min, resulting in a molar ratio of NH$_3$ to EtOH of 3. Thus, the experiments were performed in excess ammonia. The hydrogen flow rate was varied between 0 and 80 (NTP)ml/min with nitrogen as a balance, keeping the partial pressures of ammonia and ethanol in the feed constant at 6.8 and 2.3 kPa, respectively. For a hydrogen flow of 80 ml (NTP)/min, the molar ratio of EtOH:NH$_3$:H$_2$ was 2:7:80. Most experiments were performed using 165 mg of 9.2 wt% Co/SiO$_2$. In this case, the weight hourly space velocity (WHSV) of ethanol was 1.5 g$_{EtOH}$/g$_{cat}$ h, corresponding to a contact time of 0.2 s for ethanol. Before each experiment, the catalyst precursor was reduced in situ in pure hydrogen (60 ml (NTP)/min) at 500 °C for 9 h. Deviating reaction and reduction conditions are given where appropriate.

The products were analyzed using an online gas chromatograph (HP 6890 with a flame ionization detector) equipped with a six-port valve. A 30 m × 0.32 mm i.d. capillary column with a 1 μm phenylsiloxan/methylsiloxan film was used for separation. Due to the complexity of the product mixture, two sets of gas chromatography programs, adapted for proper separation of nitrogen-containing products and hydrocarbons, were used for complete analysis. The product identification was confirmed by a HP 6890 gas chromatograph with a mass-sensitive detector.

2.4. TPR as a postreaction treatment

Postsynthesis characterization of some catalysts was performed by TPR. For this purpose, the catalysts were cooled after the reaction to 100 °C, and the reaction apparatus and the reactor were flushed with hydrogen for at least 20 min. Then the temperature was increased to 700 °C at a rate of 10 °C/min, and the compounds desorbed in hydrogen flow during the TPR were analyzed by mass spectrometry using an Omnistar GSD 300O (Pfeiffer Vacuum) equipped with a Prisma QMS 200 quadrupol mass spectrometer.

3. Results and discussion

3.1. Catalyst characterization

Table 1 shows the cobalt content as determined by AAS for the prepared catalysts. The measured cobalt content is in good agreement with the amounts adjusted during the synthesis. The cobalt recovery rate was between 90 and 98%. Fig. 1 presents the results of the TPR of the oxidized catalysts. The profiles are typical for supported cobalt on silica [13] containing Co$_3$O$_4$. The reduction of Co$_3$O$_4$ is believed to proceed stepwise, because Co$_3$O$_4$ contains Co^{2+} and Co^{3+} ions [14]:

$$Co_3O_4 + H_2 \rightarrow 3CoO + H_2O, \tag{1}$$

$$3CoO + 3H_2 \rightarrow 3Co + 3H_2O. \tag{2}$$
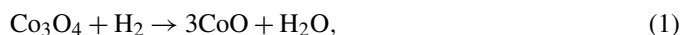
Consequently, the TPR spectra show two main peaks of hydrogen consumption. The first peak at approximately 300 °C represents the reduction step of Co$_3$O$_4$ to cobalt(II) oxide [Eq. (1)]; the second peak, which extends over a wider temperature range, can be assigned to the reduction of CoO to metallic cobalt. All investigated catalyst samples showed these two peaks, with the second peaks always being the largest. This is in agreement with the fact that the second reduction step requires a threefold greater amount of hydrogen, although it should be noted that the measured ratio of the two peaks is always <3. This ratio increases with increasing cobalt loading (from 1.2

Table 1
Determination of cobalt content of Co/SiO$_2$ catalysts synthesized by impregnation

Cobalt content adjusted in synthesis (wt%)	Cobalt content found by AAS (wt%)	Cobalt recovery rate (%)
1	0.9	90
5	4.9	98
10	9.2	92
15	14.3	95
20	18.6	93

for 0.9 wt% Co/SiO$_2$ to 2.4 for 18.6 wt% Co/SiO$_2$). This may be attributed to the increased formation of (weakly interacting) cobalt–silica species with decreasing cobalt concentration. The reduction of all catalysts was not complete at temperatures below 650 °C. Thus, at a reduction temperature of 500 °C, which was the typical reduction temperature before the hydroamination, catalysts with different cobalt loadings were reduced to different extents. A higher reduction temperature was not applied, to prevent metal sintering.

3.2. Hydroamination of ethanol

The hydroamination of ethanol yielded the amines monoethylamine (MEA), diethylamine (DEA), and triethylamine (TEA). Acetonitrile (ACN) and *N*-ethylideneethylamine (diethylimine [DEI]) were identified as other nitrogen-containing side products by mass spectroscopy. It might be assumed that the latter two products are formed by dehydrogenation of monoethylamine and diethylamine, respectively (see Scheme 3). The formation of equivalent dehydrogenation products was reported previously [7,10]. In addition to the nitrogen-containing products, up to 14 mol% of hydrocarbon was formed during hydroamination. Methane, ethane, ethane, and even propane and propene were identified as the hydrocarbon products. The formation of hydrocarbons was been mentioned previously [10,11], but the high yield and the wide variety of the hydrocarbons was surprising. Their formation was investigated to find ways to suppress them, because hydrocarbons can be major byproducts of hydroamination. In general, the product distribution of hydroamination depends on the molar ratio of ethanol and ammonia, hydrogen partial pressure, temperature, and the cobalt loading of the catalyst. The selectivity of the hydrocarbons is particularly influenced by the reaction temperature and cobalt loading on the catalyst.

3.3. Formation of hydrocarbons

Fig. 2 shows the results for the hydroamination of ethanol with ammonia at 210 °C for silica-supported catalysts with a cobalt loading of 1 to 20 wt% after 30 min time on stream. The ethanol conversion over these catalysts ranged from 35 to 50 mol%. The observed variation in the conversion can be attributed to differences in the reduced metal surface area of the catalysts, due to the variation in the cobalt loading, reducibility, and cobalt metal dispersion accompanying various cobalt loadings [2]. The amine selectivity decreased with increasing cobalt loading, accompanied by an increase in hydrocarbon selectivity. The selectivity for acetonitrile and diethylimine was low for all catalysts. In essence, the observed trend in the change of selectivity of hydrocarbons correlated with the variation in conversion; higher conversion resulted in higher selectivity for the formation of hydrocarbons at the expense of amine selectivity.

A similar correlation of amine and hydrocarbon selectivity was also observed with variation of the reaction temperature between 130 and 300 °C for the hydroamination of ethanol over 9.2 wt% Co/SiO$_2$ using a feed comprising EtOH, NH$_3$, H$_2$, and
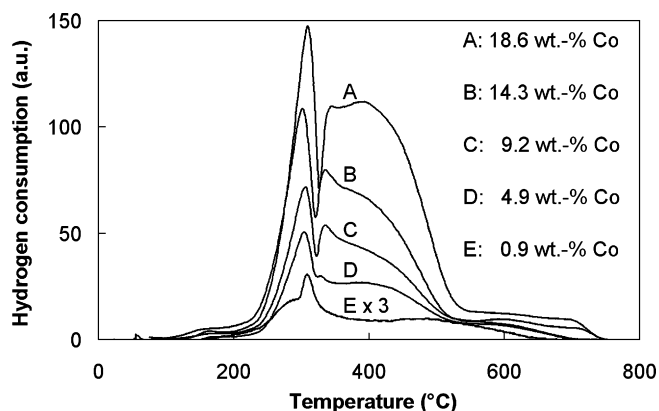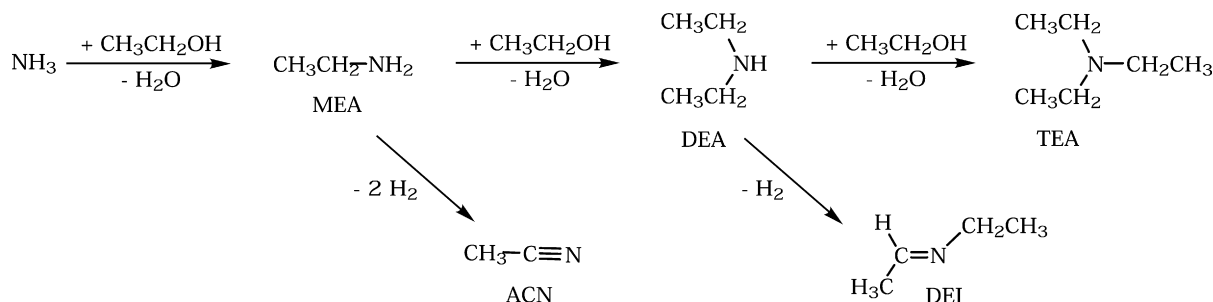

Fig. 1. Temperature-programmed reduction of Co$_3$O$_4$/SiO$_2$ catalyst precursors with different cobalt loadings.
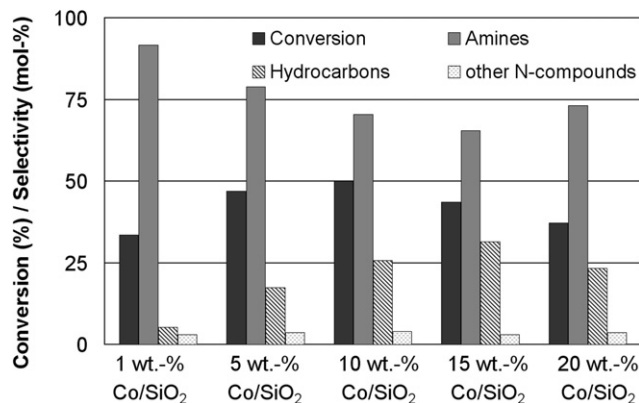

Fig. 2. Influence of cobalt loading on conversion and selectivity at 210 °C over silica supported cobalt. Molar ratio EtOH:NH$_3$:H$_2$:N$_2$ = 2:7:80:14, WHSV = 1.5 g$_{EtOH}$/g$_{cat}$ h (for 0.9 wt% Co/SiO$_2$ WHSV = 0.6 g$_{EtOH}$/g$_{cat}$ h; other *N*-compounds are acetonitrile and diethylimine).

Scheme 3. Consecutive reactions for formation of ethylamines and corresponding reduction products.
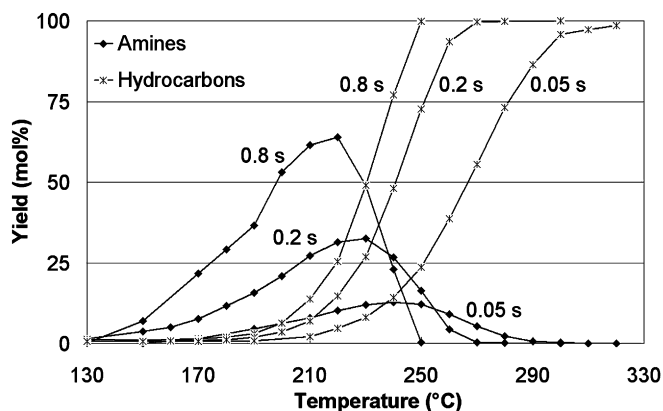
Fig. 3. Effect of reaction temperature on the hydroamination of ethanol over 9.2 wt% Co/SiO_2. All measurements after 30 min t.o.s. at the given conditions. Molar ratio $EtOH:NH_3:H_2:N_2 = 2:7:80:14$.

Fig. 4. Hydrocarbon selectivity over 9.2 wt% Co/SiO_2 as a function of f reaction temperature. Contact time = 0.2 s. Molar ratio $EtOH:NH_3:H_2:N_2 = 2:7:80:14$. All measurements after 30 min t.o.s. at the given conditions.

N_2 at a molar ratio of 2:7:80:14. The effect of reaction temperature was investigated at different space velocities ranging from 0.38 to 8 g_{EtOH}/g_{cat} h by varying the catalyst mass, resulting in contact times between 0.8 and 0.05 s. These experiments started at 130 °C, and the temperature was increased by 10 °C every 30 min, with each sample obtained immediately before the next temperature increase. Taking into account the contact time of <1 s, the chosen time range of 30 min should be sufficiently long to obtain steady-state conditions at the next temperature level. Identical results were obtained by decreasing the temperature stepwise from 300 °C. Thus, catalyst deactivation did not falsify these results, legitimating the use of a single catalyst sample for the entire temperature range.

Fig. 3 shows the yields of amines and hydrocarbons as a function of temperature at the three different contact times. Contact time strongly affected the amount of amines formed relative to the amount of hydrocarbons formed. An increase in the contact time (and thus a decrease in the space velocity) at a particular temperature was accompanied by an increase in the hydrocarbon yield. The influence of contact time on the distribution of amines and hydrocarbons shows that this distribution is kinetically controlled. At higher reaction temperatures, the amount of hydrocarbons formed relative to the amount of amines formed increases. The reaction temperature, at which exclusively the formation of hydrocarbons is observed, decreases with increasing contact time. For instance, at a contact time of 0.05 s, a temperature above 300 °C is required to observe the exclusive formation of hydrocarbons, whereas at a contact time of 0.8 s, this occurs at temperatures above 250 °C. The increased hydrocarbon selectivity with increasing contact time indicates a consecutive pathway, that is, formation from the primary products of hydroamination. This conclusion is in accordance with previous proposals for the formation of hydrocarbons via hydrogenolyses of amines [10,11].

Fig. 4 shows the selectivity of the individual hydrocarbon compounds as a function of reaction temperature at a contact time of 0.2 s over 9.2 wt% Co/SiO_2 using a feed comprising EtOH, NH_3, H_2, and N_2 at a molar ratio of 2:7:80:14. The saturated hydrocarbons methane, ethane, and propane were the main representatives of this group of products, and at 300 °C,
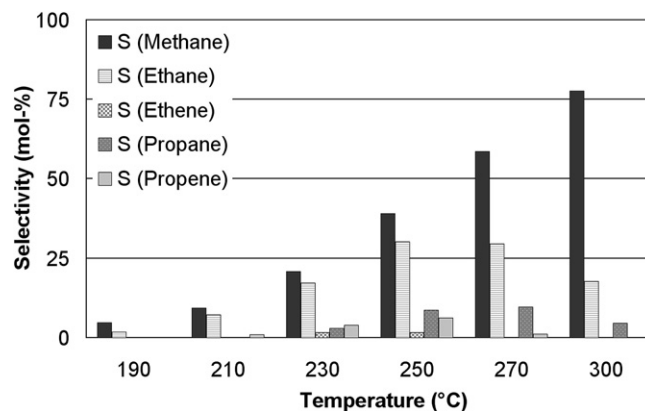
the molar ratio of methane:ethane:propane was 17:4:1. In addition, ethene and propene were formed at temperatures above 210 °C, reaching their maximum selectivity at 250 °C. The formation of methane and C_3-hydrocarbons requires C–C-bond fission and coupling. The high molar methane content indicates a rather facile fission of the C–C bond. The absence of methylamines in the product stream would indicate C–C fission in a C_2-hydrocarbon surface species formed on hydrogenolysis of ethylamines. The surface C_1 species can then recombine to form longer-chain hydrocarbons, such as C_3 hydrocarbons, in a process similar to the Fischer–Tropsch process [15,16]. It should be noted, however, that the observed molar ratio of C_2 hydrocarbons to methane in the hydroamination of ethanol was larger than that of C_3 hydrocarbons to C_2 hydrocarbons. The opposite was observed in the Fischer–Tropsch synthesis [16]. This may be explained by a dual reaction pathway for the formation of C_2 hydrocarbons, that is, through desorption of C_2 surface species formed directly from ethanol, as proposed by Jones et al. [5] and Jackson et al. [6], on the hydrogenolysis of ethylamines and through desorption of C_2 surface species generated through a chain growth process.

Because hydrocarbons are undesired byproducts, efforts were taken to decrease their selectivity while maintaining a high level of ethanol conversion. It was found that the degree of reduction of the cobalt catalyst is an important factor in the production of the hydrocarbons. Fig. 5 shows the ethanol conversion and the hydrocarbon selectivity as a function of reaction temperature for a 0.9 wt% Co/SiO_2 catalyst reduced before the reaction in 60 ml (NTP)/min hydrogen at different reduction conditions: 1 h at 300 °C, 14 h at 350 °C, 14 h at 500 °C, and 14 h at 600 °C. The four samples had different degrees of reduction (cf. TPR spectra of the 0.9 wt% Co/SiO_2 catalyst in Fig. 1); however, similar levels of ethanol conversion were obtained for samples reduced at temperatures below 500 °C (Fig. 5). The sample reduced at 600 °C showed a lower ethanol conversion, which might be explained by sintering of the cobalt metal and the simultaneous decrease in the active metal surface [2]. The selectivity of the hydrocarbons decreased with increasing applied reduction temperature. At a reaction temperature of 250 °C, the selectivity of hydrocarbons was 10 mol%
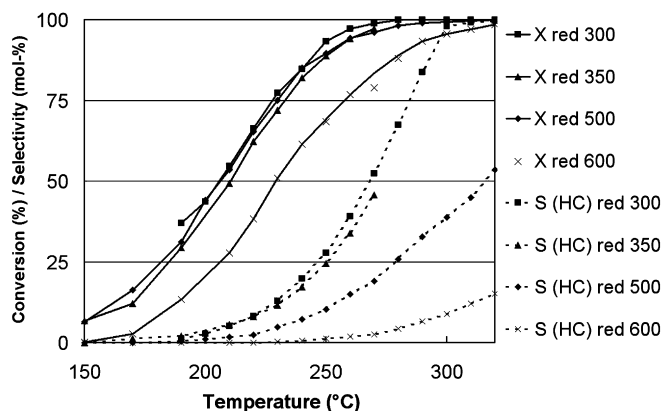
Fig. 5. Ethanol conversion and selectivity of hydrocarbons as a function of reaction temperature on 0.9 wt% Co/SiO$_2$ reduced at different conditions. All measurements after 30 min t.o.s. at the given conditions: WHSV = 0.75 g$_{EtOH}$/g$_{cat}$ h; molar ratio EtOH:NH$_3$:H$_2$:N$_2$ = 2:7:80:14.

when the catalyst was reduced at 500 °C and 25 mol% after reduction at 350 °C at similar levels of ethanol conversion. Thus, it may be concluded that the secondary formation of hydrocarbons is correlated with the amount of nonreduced cobalt sites in the catalyst. The enhanced hydrocarbon formation might be directly or indirectly related to the number of sites comprising of nonreduced cobalt present in the catalyst. A direct correlation would have been be obtained had these sites catalyzed amine hydrogenolysis. Sewell et al. [2] proposed that acidic sites in the catalysts, present as, for example, an unreduced Co^{2+} support compound, are responsible for disproportionation reactions, particularly those yielding monoethylamine, which may exhibit higher reactivity for hydrogenolysis. This would lead to an indirect correlation with the number of nonreduced cobalt sites.

3.4. Deactivation of the cobalt catalyst

A long-duration experiment at 210 °C was performed with a switchover from hydrogen to nitrogen (see Figs. 6 and 7) to gain more insight in the effect of catalyst deactivation and the effect of hydrogen on product selectivity. Under the reaction conditions used (with a reduced space velocity of 0.75 g$_{EtOH}$/g$_{cat}$ h), formation of the amines MEA, DEA, and TEA, along with hydrocarbons and diethylimine, was observed. Acetonitrile as a product could not be detected in the presence of hydrogen.

Figs. 6 and 7 show that the conversion of ethanol and the selectivity of amines decreased at the beginning of the reaction, reaching steady-state conditions after 5 h time on stream. Whereas ethanol conversion decreased from 52 to 45%, amine selectivity decreased from 75 to 72 mol% with a concomitant increase in the hydrocarbon selectivity. The substitution of hydrogen by nitrogen completely changed the reaction behavior of the cobalt catalyst; conversion dropped from 45 to 11%. Acetonitrile was the only product, with amines, diethylimine, and hydrocarbons no longer formed. During reaction in nitrogen atmosphere, the conversion of ethanol decreased continuously, dropping to <1% after 20 h on stream. The deactivation is fully reversible; switching from nitrogen again to hydrogen after 44 h
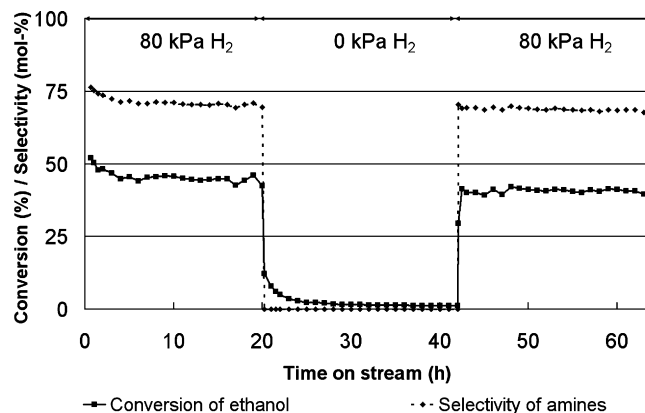

Fig. 6. Long-duration experiment with switchover from hydrogen to nitrogen on 9.2 wt% Co/SiO$_2$ at 210 °C. WHSV = 0.75 g$_{EtOH}$/g$_{cat}$ h; molar ratio EtOH:NH$_3$:H$_2$:N$_2$ = 2:7:80:14, 2:7:0:94, respectively.
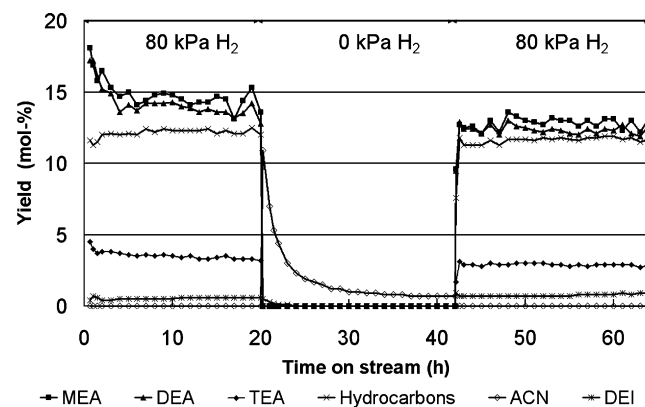

Fig. 7. Yields of all products in a long-duration experiment with switchover from hydrogen to nitrogen. Conditions like in Fig. 6. Hydrocarbons include ethane and ethene.

on stream restored the original activity within 30 min. This activity remained nearly constant for another 20 h on stream.

Two main deactivation phenomena were observed: (i) deactivation in the presence of hydrogen in the first few hours, which can be explained by deactivation of the most active catalytic sites by irreversible adsorption of educts or products and their decomposition to carbonaceous species or carbon deposits, and (ii) collapse of the catalyst activity when hydrogen was eliminated from the feed. This rapid drop in catalyst activity and its reversibility were previously ascribed to the formation of cobalt nitrides, which can be formed by ammonia in the absence of hydrogen [11,12].

A postsynthesis characterization was performed in 9.2 wt% Co/SiO$_2$ samples that had been used in the hydroamination of ethanol at 210 °C in hydrogen and nitrogen atmosphere, respectively. Before the temperature ramp, hydrogen was flushed for at least 20 min at 100 °C through the reactor. Methane was the only product that evolved during TPR (see Fig. 8), indicating gasification of carbonaceous species on the catalyst surface. Methane evolution was seen in two temperature ranges. A first peak of methane was observed at approximately 260 °C, which is slightly higher than the reaction temperature. This peak can be ascribed to reaction intermediates that remained at reaction
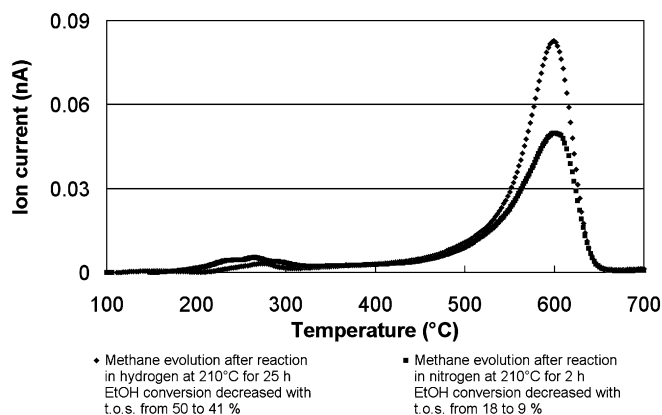
Fig. 8. Methane evolution in postsynthesis temperature-programmed reduction of 9.2 wt% Co/SiO$_2$. Molar ratio EtOH:NH$_3$:H$_2$:N$_2$ = 2:7:80:14 and 2:7:0:94, respectively.

Fig. 9. TPR of 9.2 wt% Co/SiO$_2$ after treatment with 25 vol% ammonia.

conditions on the cobalt surface due to strong adsorption. A second peak of methane evolution was detected at around 600 °C. At these temperatures, carbon deposits and strongly bonded carbonaceous species can be hydrogenated to methane. The latter species can accumulate with time on stream and may cause irreversible catalyst deactivation.

Nitrogen-containing compounds and water were not detected during these experiments, indicating the absence of nitrogen- and oxygen-containing species in the catalyst. The absence of nitrogen-containing compounds is surprising, because a strong surface poisoning effect was observed when the reaction was performed in a nitrogen atmosphere instead of a hydrogen atmosphere (see Figs. 6 and 7). This effect was ascribed to the interaction between ammonia and the cobalt surface, for example, the formation of cobalt nitrides.

Because no evidence of nitrogen was found on the deactivated catalyst, two experiments with ammonia were performed, to evaluate whether the applied TPR experiment is feasible for detecting nitrogen-containing cobalt species. A catalyst containing 9.2 wt% Co was treated at 310 °C for 25 h with a mixture of 25 vol% of ammonia in hydrogen and nitrogen, respectively [20 ml (NTP)/min]. This temperature and reaction time should have allowed the formation of cobalt–nitrogen surface compounds. After this treatment, the catalyst was cooled to 70 °C, and the ammonia flow was turned off. Pure hydrogen was passed through the reactor for approximately 15 min, simulating the isothermal step at the beginning of each TPR experiment. Subsequently, the temperature was increased at a rate of 10 °C/min (Fig. 9). After treatment of the catalyst in a NH$_3$/H$_2$ mixture, no products could be detected in the TPR, indicating the absence of strongly adsorbed nitrogen-containing surface species and the absence of cobalt nitride if hydrogen was present. This finding demonstrates that the ammonia–catalyst interaction is not responsible for deactivation in the presence of hydrogen. Ammonia was observed in the H$_2$-TPR of the catalyst treated in NH$_3$/N$_2$, indicating the presence of chemisorbed ammonia or cobalt nitride on the catalyst surface and explaining its deactivation. Interestingly, the release of ammonia occurred immediately after the switchover to hydrogen at 70 °C. Thus, the absence of nitrogen-containing species in the TPR
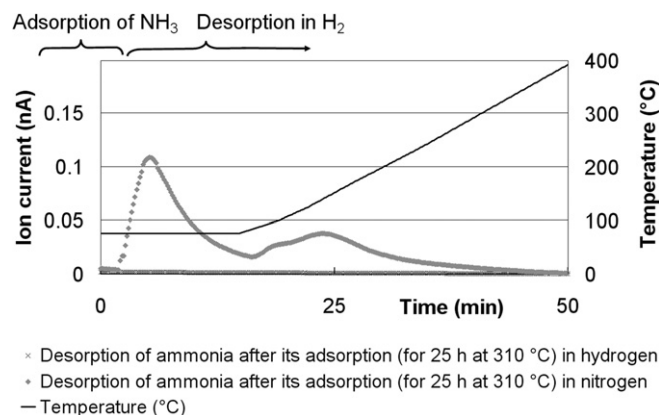
experiment of the spent catalyst (Fig. 8) can be explained by the immediate release of adsorbed nitrogen species during the isothermal step at 100 °C in hydrogen atmosphere. This finding demonstrates that the interaction of ammonia with the catalyst is rather weak and can be enduring only in the absence of hydrogen.

4. Conclusion

During the hydroamination of ethanol, such products as acetonitrile, diethylimine, methane, ethene, ethane, propane, and propene have been identified along with the three desired ethylamines. The formation of hydrocarbons can be explained by catalytic fragmentation of the ethylamines through the generation of ethyl and ethylidene species, followed by carbon–carbon bond fission and coupling.

The formation of hydrocarbons depends on the pretreatment of the applied catalyst. Catalysts reduced at higher temperatures exhibit lower hydrocarbon production. This is indirectly ascribed to the greater catalyst reduction. Oxidic cobalt species are thought to catalyze amine disproportionation reactions, yielding more monoethylamine, which has the highest reactivity for hydrogenolysis.

Ethanol conversion and selectivity depend strongly on the presence of hydrogen. Without hydrogen, a reversible deactivation occurs that can be ascribed to a ammonia–cobalt interaction, such as strong chemisorption or formation of nitrides. Carbon-containing species and carbonaceous deposits result in decreased catalyst activity as well. They also are formed in hydrogen as well as in nitrogen atmosphere, as demonstrated by TPR.

In summary, high selectivity of ethylamines was obtained with silica-supported cobalt catalysts at high hydrogen partial pressures and low temperatures using highly reduced catalysts.

References

[1] G. Heilen, H.J. Mercker, D. Frank, R.A. Reck, R. Jäck, in: W. Gerhertz (Ed.), Ullmanns Encyclopedia of Industrial Chemistry, vol. 2A, fifth ed., VCH, Weinheim, 1985, pp. 1–18.

[2] G.S. Sewell, C.T. O'Connor, E. van Steen, J. Catal. 167 (1997) 513–521.

[3] T. Mallat, A. Baiker, in: G. Ertl, W.L. Knözinger, J. Weitkamp (Eds.), Handbook of Heterogeneous Catalysis, vol. 5, VCH, Weinheim, 1997, pp. 2334–2339.

[4] G. Sewell, C. O'Connor, E. van Steen, Appl. Catal. A 125 (1995) 99–112.

[5] J.R. Jones, A.P. Sharratt, S.D. Jackson, L.F. Gladden, G. Webb, in: J. Allen (Ed.), Synthesis and Applications of Isotopically Labeled Compounds, 1994, vol. 5, Wiley, New York, 1995, pp. 751–759.

[6] S.D. Jackson, J.R. Jones, A.P. Sharratt, L.F. Gladden, R.J. Cross, G. Webb, Chem. Ind. 89 (2003) 453–460.

[7] A. Baiker, W. Caprez, W.L. Holstein, Ind. Eng. Chem. Prod. Res. Dev. 22 (1983) 217–225.

[8] H. Cheng, J.W. Mitchell, K.S. Hayes, in: NATO Science Series II: Mathematics, Physics and Chemistry, vol. 68, 2002, pp. 385–403.

[9] J.M. Pommersheim, J. Coull, AIChE J. 17 (1971) 1075–1080.

[10] J.R. Anderson, N.J. Clark, J. Catal. 5 (1966) 250–263.

[11] A. Baiker, D. Monti, Y.S. Fan, J. Catal. 88 (1984) 81–88.

[12] A. Baiker, Ind. Eng. Chem. Prod. Res. Dev. 20 (1981) 615–618.

[13] E. van Steen, G.S. Sewell, R.A. Makhote, C. Micklethwaite, H. Manstein, M. de Lange, C.T. O'Connor, J. Catal. 162 (1996) 220–230.

[14] B. Viswanathan, R. Gopalakrishnan, J. Catal. 99 (1986) 342–348.

[15] M.E. Dry, Appl. Catal. A 138 (1996) 319–344.

[16] M. Claeys, E. van Steen, Stud. Surf. Sci. Catal. 152 (2004) 601–680.